Retinal Microglial Activation and Inflammation Induced by Amadori-Glycated Albumin in a Rat Model of Diabetes

Ahmed S. Ibrahim,[1,2,3] Azza B. El-Remessy,[1,2,4,5] Suraporn Matragoon,[4,5] Wenbo Zhang,[6] Yogin Patel,[7] Sohail Khan,[1] Mohammed M. Al-Gayyar,[3,4,5] Mamdouh M. El-Shishtawy,[3] and Gregory I. Liou[1,2]

OBJECTIVE—During diabetes, retinal microglial cells are activated to release inflammatory cytokines that initiate neuronal loss and blood–retinal barrier breakdown seen in diabetic retinopathy (DR). The mechanism by which diabetes activates microglia to release those inflammatory mediators is unclear and was therefore elucidated.

RESEARCH DESIGN AND METHODS—Microglia activation was characterized in streptozocin-injected rats and in isolated microglial cells using immunofluorescence, enzyme-linked immunosorbent assay, RT-PCR, and Western blot analyses.

RESULTS—In 8-week diabetic retina, phospho-extracellular signal–related kinase (ERK) and P38 mitogen-activated protein kinases were localized in microglia, but not in Mueller cells or astrocytes. At the same time, Amadori-glycated albumin (AGA)-like epitopes were featured in the regions of microglia distribution, implicating a pathogenic effect on microglial activation. To test this, diabetic rats were treated intravitreally with A717, a specific AGA-neutralizing antibody, or murine IgG. Relative to nondiabetic rats, diabetic rats (IgG-treated) manifested 3.9- and 7.9-fold increases in Iba-1 and tumor necrosis factor (TNF)-α mRNAs, respectively. Treatment of diabetic rats with A717 significantly attenuated overexpression of these mRNAs. Intravitreal injection of AGA per se in normal rats resulted in increases of Iba-1 expression and TNF-α release. Guided by these results, a cultured retinal microglia model was developed to study microglial response after AGA treatment and the mechanistic basis behind this response. The results showed that formation of reactive oxygen species and subsequent activation of ERK and P38, but not Jun NH2-terminal kinase, are molecular events underpinning retinal microglial TNF-α release during AGA treatment.

CONCLUSIONS—These results provide new insights in understanding the pathogenesis of early DR, showing that the accumulated AGA within the diabetic retina elicits the microglial activation and secretion of TNF-α. Thus, intervention trials with agents that neutralize AGA effects may emerge as a new therapeutic approach to modulate early pathologic pathways long before the occurrence of vision loss among patients with diabetes.
***Diabetes* 60:1122–1133, 2011**

From the [1]Department of Ophthalmology, Medical College of Georgia, Augusta, Georgia; the [2]Vision Discovery Institute, Medical College of Georgia, Augusta, Georgia; the [3]Department of Biochemistry, Faculty of Pharmacy, Mansoura University, Mansoura, Egypt; the [4]Program in Clinical and Experimental Therapeutics, University of Georgia, Athens, Georgia; the [5]VA Medical Center, Augusta, Georgia; the [6]Vascular Biology Center, Medical College of Georgia, Augusta, Georgia; and the [7]Department of Medicine, Medical College of Georgia, Augusta, Georgia.

Corresponding author: Gregory I. Liou, giliou@mcg.edu.

Received 16 August 2010 and accepted 6 January 2011.

DOI: 10.2337/db10-1160

This article contains Supplementary Data online at http://diabetes.diabetesjournals.org/lookup/suppl/doi:10.2337/db10-1160/-/DC1.

During the past decade, it has become clear that inflammation is a key feature in diabetes that leads to long-term complications in specific organs, in particular the eye and kidney (1). In the eye, the major complication is diabetic retinopathy (DR), which is the leading cause of blindness in the western world and affects approximately three fourths of diabetic patients within 15 years after onset of the disease (2). The recommended treatment for these patients has been laser photocoagulation, which is an invasive procedure with considerable limitations and adverse effects. Therefore, there is a great need for the development of new noninvasive therapies to treat those affected by DR. These therapies can be discovered by unraveling the pathophysiology of DR.

As a consequence of diabetes, retinal microglia, a subtype of glial-immune sentinel cells prestationed in the tissue, become reactive, leading to the release of soluble cytotoxins that contribute to neuronal and vascular cell death and ultimately the progression of DR (3). However, the underlying mechanism of microglial activation during diabetes is still incompletely understood.

In recent years, human and animal studies have elucidated that many effects of hyperglycemia are mediated by glycated proteins (4). Amadori-glycated albumin (AGA) is the prominent form of circulating glycated proteins in vivo, and its concentration is significantly increased after diabetes, reaching its maximum in 5–7 weeks (5). AGA arises from the nonenzymatic condensation reaction between a reducing sugar and susceptible amino groups. This modification confers properties to AGA that are not possessed by the native, nonglycated albumin, such as the promotion of the inflammatory response and the activation of different mitogen-activated protein kinase (MAPK) cascades in several cell types (6–9). These MAPKs, including extracellular signal–related kinase (ERK), Jun NH2-terminal kinases (JNKs), and P38, can be independently or simultaneously activated depending on the target cells (8–10).

On the basis of these properties of AGA, a growing body of evidence now supports the causal role of AGA in the development of many complications associated with diabetes (11–13). In relation to DR, elevated AGA has been documented in the retinal capillaries of diabetic patients with retinopathy (14) and in the retina of diabetic rats (15). Treatment of diabetic *db/db* mice with A717 antibody, which specifically recognizes AGA, ameliorated retinal basement membrane thickening (16). Furthermore, treatment of diabetic rats with 2-(3-chlorophenylamino)-phenylacetic acid, which inhibits the nonenzymatic glycation of albumin, mitigated vitreous changes in angiogenic cytokines associated with the development of DR (17). Therefore, AGA is believed to possess biologic characteristics that are linked to

the DR pathogenesis and might be involved in the activation of retinal microglia. In the present work, we aimed to study the ability of AGA to induce retinal microglial activation and their secretion of inflammatory cytokines both in vivo and in vitro.

RESEARCH DESIGN AND METHODS

All procedures with animals were performed in accordance with the Association for Research in Vision and Ophthalmology Statement for the Use of Animals in Ophthalmic and Vision Research and Medical College of Georgia guidelines. Diabetes was induced in male SD rats by intravenous injection of streptozocin (STZ) (60 mg/kg) and confirmed by urine-glucose levels >350 mg/dL. Eyes were used for immunofluorescence or Western examination at 8 weeks of diabetes. For intravitreal injections, the procedure was essentially the same as previously described (18). The A717 intravitreal injection scheme was chosen on the basis of certain assumptions regarding the estimated amount of AGA to be neutralized. We estimated rat vitreous volume at 50 μL (19), with AGA concentration of 1.9 μg/mL (17). This would correspond with an approximate total vitreous AGA of 0.09 μg. On a stoichiometric basis, it would require ~0.2 μg antibody (mol wt ~150 kD) to neutralize ~0.09 μg of AGA (mol wt ~66.5 kD). First, A717 injections were given at 10 days, and a booster dose was given at 7 weeks of diabetes. These two time points were selected presumably because the former represents the earliest occurrence of AGA, whereas the latter marks its maximum accumulation (5).

Microglia culture. Microglia were isolated from retinas of newborn SD rats according to a previous procedure (20). Cell viability after various drug treatments was determined by counting the number of trypan blue-excluding cells using a hemocytometer.

AGA preparation. AGA was purchased from Sigma-Aldrich Co. (St. Louis, MO), purified by affinity chromatography on phenylboronate resin, concentrated, and desalted into PBS. This preparation contains 2.2-mol hexose-lysine/mol-albumin, but fluorescent advanced glycation end products (AGEs) were not detectable and the major AGE *N*-(carboxymethyl) lysine was present in only minute amounts (21). The concentration of AGA (500 μg/mL) chosen in our study is close to what has been used previously to study other glycated albumin-mediated responses (22) and represents those found in clinical specimens (23). The specificity of AGA activity was determined by neutralization with its antibody, A717. Briefly, AGA or BSA was balanced with PBS at pH = 7.4, kept overnight at 4°C on a rocker with A717 antibody or IgG, served as a control, and followed by the addition of A/G agarose beads. The beads were then removed by centrifugation, and the supernatant was collected and used for microglia treatment. The endotoxin level was checked by an endotoxin testing kit (Limulus amebocyte assay, E-Toxate, Sigma-Aldrich Co.). Alternatively, AGA was purchased from Exocell Inc. (Philadelphia, PA). This alternative product contains 1-mol hexose-lysine/mol-albumin and was purified by boronate-affinity column and Detoxi-Gel Endotoxin Removal Gel. Viability of cells after AGA-treatment was checked by transferase-mediated dUTP nick-end labeling assay (Trevigen Inc., Gaithersburg, MD) following the manufacturer's instructions.

Immunofluorescence. Dual-labeled immunofluorescence analysis was performed using frozen retinal sections. Briefly, sections were fixed in 4% paraformaldehyde, blocked with 10% normal goat serum, and then incubated with primary antibodies (Table 1) overnight. Thereafter, sections were briefly washed with PBS and incubated with appropriate secondary antibodies (Table 1). Slides were examined by confocal microscopy (LSM 510, Carl Zeiss AG, Oberkochen, Germany). Specificity of the reaction was confirmed by omitting the primary antibody. Images were collected from five sections per rat of at least four to six rats per group.

RNA interference. Microglial cells were transfected with ERK or control small interfering (si)RNAs (Ambion, Austin, TX) using HiPerFect (Qiagen, Venlo, the Netherlands) per the manufacturer's instructions.

Quantitative real-time PCR. Total RNA was isolated from rat retina using a Promega kit (Promega Corp., Madison, WI). Subsequently, cDNAs were generated from 1 μg of total RNA, using the High-Capacity cDNA Reverse Transcription Kit (Applied Biosystems, Foster City, CA), and subjected to a 40-cycle PCR amplification. The ready-made primer and probe sets were ordered from Applied Biosystems (Catalog: Iba-1: Rn01525935_m1; TNF-α: Rn99999017_m1; 18S: Hs03003631_g1). Three replicates were run for each gene for each sample in a 96-well plate. *18S* was used as the endogenous reference gene.

Western blot analysis. Cell or retinal lysates were subjected to Western blot analysis using antibodies specified in Table 1 according to a previous procedure (20).

ELISA assay. Tumor necrosis factor (TNF)-α levels in the rat vitreous or supernatants of culture media were estimated with ELISA kit (R&D Systems Inc., Minneapolis, MN) per the manufacturer's instructions (20).

DCF assay for reactive oxygen species formation. DCF, the oxidation product of the reagent 2`,7`-dichlorofluorescin diacetate, was used as a marker of cellular oxidation according to a previous procedure (20).

Data analysis. The results were expressed as mean ± SD. Differences among experimental groups were evaluated by ANOVA, and the significance of differences between groups was assessed by the post hoc test (Fisher protected least significant difference) when indicated. Significance was defined as $P < 0.05$.

TABLE 1
Primary antibodies used for different experiments in this study

Antibody	Catalog no.	Vendor	Host	Working dilution	
				IF	WB
Anti-Iba1	019–19741	Wako	Rabbit	1:200	—
Anti-OX-42	201801	BioLegend (San Diego, CA)	Mouse	1:200	—
Antiphospho-ERK	9106	Cell Signaling Technology Inc. (Danvers, MA)	Mouse	1:400	1:2,000
Antiphospho-P38	4631	Cell Signaling Technology Inc.	Rabbit	1:100	1:1,000
Anti-GFAP	AB5541	Millipore (Billerica, MA)	Chicken	1:500	—
Anti-AGA	A717	Exocell Inc. (Philadelphia, PA)	Mouse	1:50	1:500
Anti-albumin	PA1–10298	Thermo Fisher Scientific (Waltham, MA)	Rabbit	—	1:2,000
Antiactin	A2066	Sigma-Aldrich Co. (St. Louis, MO)	Rabbit	—	1:2,000
Anti-ERK	9102	Cell Signaling Technology	Rabbit	—	1:1,000
Anti-P38	9212	Cell Signaling Technology	Rabbit	—	1:1,000
Antiphospho-JNK	9255	Cell Signaling Technology	Mouse	—	1:2,000
Anti-JNK	9252	Cell Signaling Technology	Rabbit	—	1:1,000
Anti-rabbit (Texas red or Oregon green)	A21072 737677	Invitrogen (Carlsbad, CA)	Goat Chicken	1:500	—
Anti-mouse (Texas red or Oregon green)	737674 A11017	Invitrogen	Chicken Goat	1:500	—
Antichicken (Cya5)	92590	Millipore	Donkey	1:500	—
Anti-rabbit HRP	7074	Cell Signaling Technology	Goat	—	1:10,000
Anti-mouse HRP	7076	Cell Signaling Technology	Goat	—	1:10,000

HRP, horseradish peroxidase; IF, immunofluorescence; WB, Western blot.

RESULTS

ERK and P38 MAPKs are selectively activated in the retinal microglia during diabetes. Recent evidence has shown that MAPK cascade is one of the attractive targets for intervention in the inflammatory-associated diseases, such as diabetes. Therefore, the role of retinal microglia and macroglia during diabetes was investigated by determining MAPK signaling in frozen eye sections. As shown in Fig. 1*A* and *B*, in the 8-week diabetic retina, numerous Iba-1- or OX-42-positive cells (activated microglia) appeared hypertrophic or amoeboid and were observed in the outer plexiform layer or ganglion cell layer, or frequently clustered around the perivascular region (Supplementary Fig. 1). In contrast, in the nondiabetic retina, these cells had oval cell bodies with ramified processes (Supplementary Fig. 2). Double immunofluorescence showed that pERK- and pP38-labeled cells were colocalized with Iba-1 or OX-42 antigen, but not with glial fibrillary acidic protein (GFAP). These results revealed that diabetes leads to characteristic glial cell changes within the retina in which activation of ERK and P38 occur in the activated microglia, but not in astrocytes or Mueller cells.

AGA is a proinflammatory trigger in diabetes-induced retinal microglial activation and inflammation. The induction of microglial reactivity is associated with a local proinflammatory environment (3,24) that could be triggered by various conditions operating in the course of diabetes. Given the fact that AGA provokes proinflammatory responses in many types of cells, including immune cells (7,9,25), we hypothesized that this glycated protein may also be implicated in diabetes-induced microglial activation and retinal inflammation. To test this, we first sought to determine whether this glycated protein is accumulated in the diabetic retina and whether this accumulation occurs in the region of microglia distribution. The results

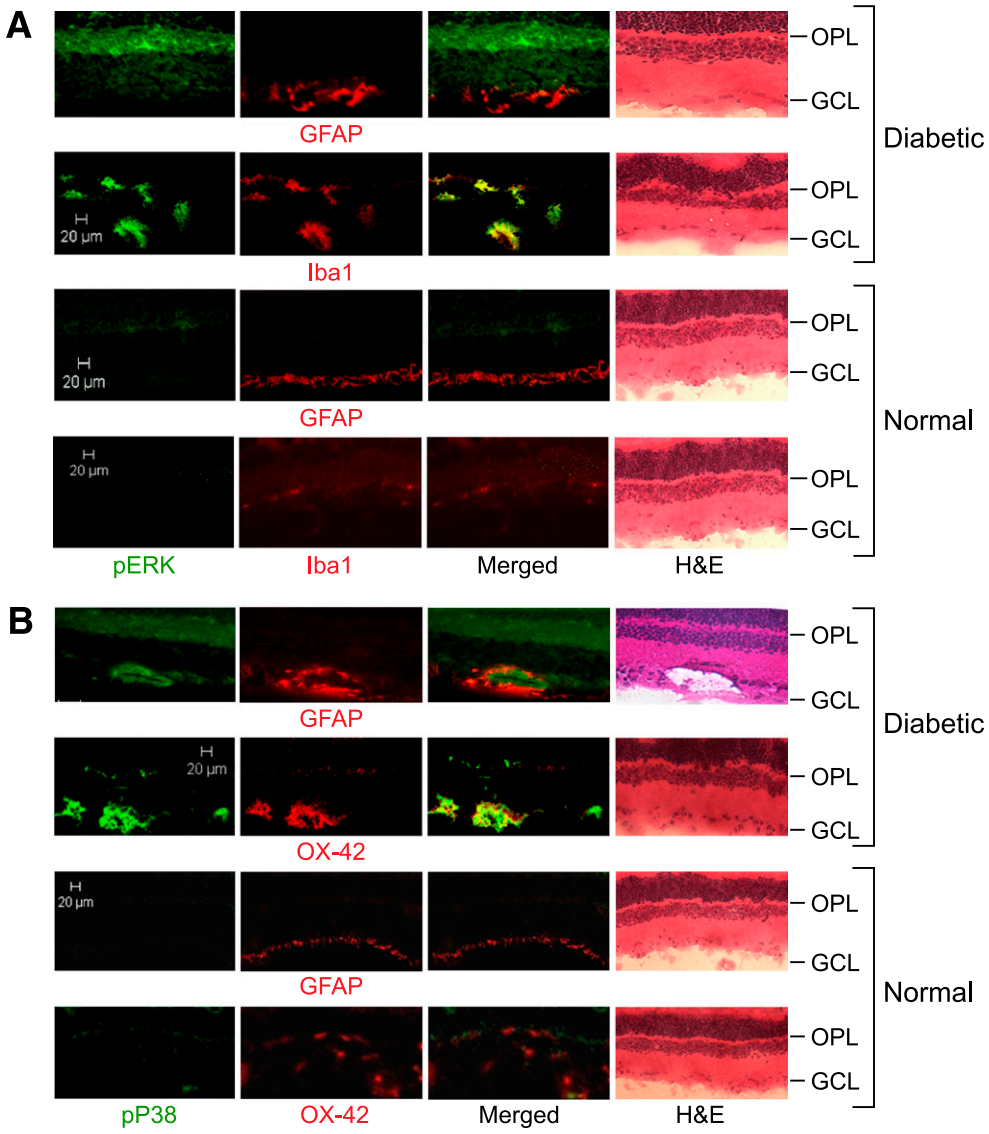

FIG. 1. Activation of ERK and P38 in diabetes occurs in the retinal microglia. Immunolabeling of phospho-ERK (green) (*A*) or phospho-P38 (green) (*B*) with Iba-1 (red) or OX-42 (red), markers of activated microglia, or with GFAP (red), a marker of astrocytes or activated Mueller cells, was made in the retinas of diabetic (8 weeks after STZ induction) and normal rats. Yellow displayed from merged red and green. Scale bar, 20 µm. GCL, ganglion cell layer. H&E, hematoxylin–eosin stain; OPL, outer plexiform layer. (A high-quality digital representation of this figure is available in the online issue.)

showed that AGA and albumin were increased approximately 4.5- and fourfold in the retina of 8-week diabetic rats compared with nondiabetic retinas (Fig. 2*A* and *B*). Moreover, AGA-like epitopes were featured within the retinal tissue of 8-week diabetic rats (Fig. 2*C*) and at 10 days after the detection of hyperglycemia (data not shown). These epitopes were found to be colocalized with the microglial marker (Fig. 2*C*), implicating a pathogenic effect on microglial function.

Second, to determine whether AGA is involved in the pathogenesis of microglial activation and inflammation during diabetes, we used two complementary approaches. In our first approach, the putative biological effect of AGA per se in retinal inflammation was investigated using an experimental model in which normal rats were injected intravitreally with AGA or nonglycated albumin. As shown in Fig. 2*D* and *E*, AGA injection induced a significant five- and 3.3-fold increase in retinal Iba1 mRNA expression and TNF-α release, respectively, compared with controls injected with nonglycated albumin.

The second approach was to assess whether neutralizing AGA biological activity in the diabetic retinas with A717

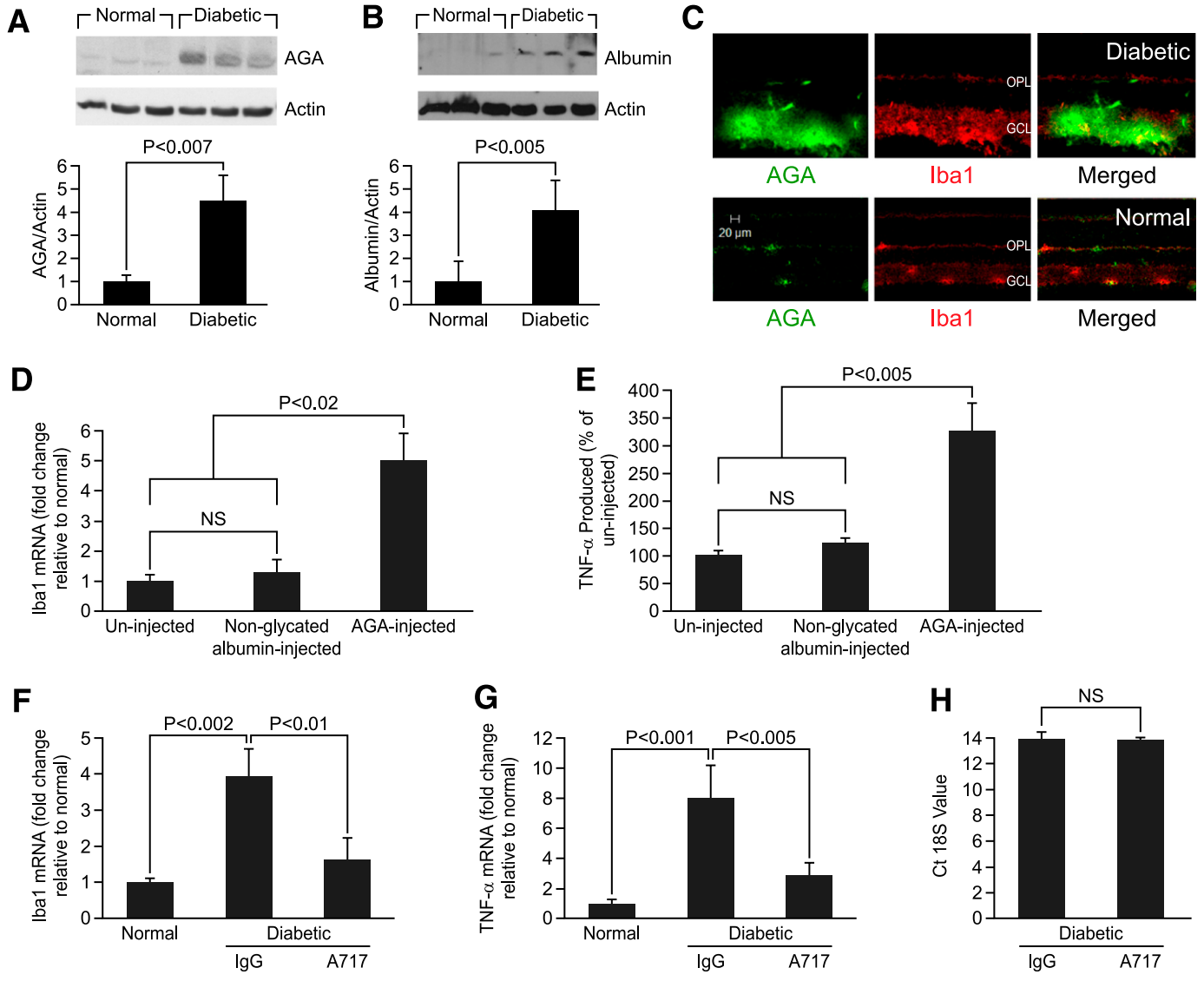

FIG. 2. AGA as a proinflammatory trigger in diabetes-induced retinal microglial activation and inflammation. *A* and *B*: AGA and albumin expression in retina of nondiabetic rats (normal) and 8-week diabetic rats, analyzed by Western blot. Ratio of the intensities of AGA or albumin relative to the actin for the patients with diabetes was compared with normal, which was arbitrarily set at 1.0. Data shown for the comparison of normal and diabetic rats are the mean ± SD and representative of four to six animals per group. *C*: Immunolabeling of AGA (green) with Iba-1 (red) in the normal and 8-week diabetic rat retinas. *D*: Activation of retinal microglia by injected AGA in normal rats. Nondiabetic rats were injected intravitreally with AGA (500 μg/mL) or equal amounts of nonglycated albumin. Retinal Iba-1 mRNA was determined by real-time PCR 24 h later. Data shown are the mean ± SD (n = 4–6). *E*: Proinflammatory effect of injected AGA in normal rat retina. Nondiabetic rats were injected intravitreally with AGA (500 μg/mL) or equal amounts of BSA. Vitreal TNF-α was determined by ELISA 24 h later. Data shown are the mean ± SD (n = 4–6). *F* and *G*: Attenuation of increased *Iba1* and *TNF-α* gene expression in diabetic rats treated with A717 or IgG. Total RNA was extracted from snap-frozen retinas, and Iba1 and TNF-α mRNAs were then determined by real-time PCR and normalized to normal nondiabetic control. Data shown are the mean ± SD (n = 4–6). *H*: Cyclic threshold values of 18S in the retina of diabetic rats treated with A717 or IgG. Data shown are the mean ± SD (n = 4–6). Ct, cyclic threshold; GCL, ganglion cell layer; OPL, outer plexiform layer. (A high-quality color representation of this figure is available in the online issue.)

would attenuate diabetes-induced retinal microglial activation and TNF-α release. As shown in Fig. 2*F* and *G*, treatment with A717 significantly decreased the elevated retinal *Iba1* and *TNF-α* gene expression observed in the IgG-treated diabetic rats by ~60 and 65%, respectively. Of note, the expression level of 18S was approximately the same among diabetic groups (Fig. 2*H*), indicating that the effect of A717 on gene expression is not due to a generalized nonspecific suppression of retinal gene expression. Taken together, these results demonstrate that the formation of AGA within the diabetic milieu is one of the major contributing factors to microglial activation and therefore retinal inflammation.

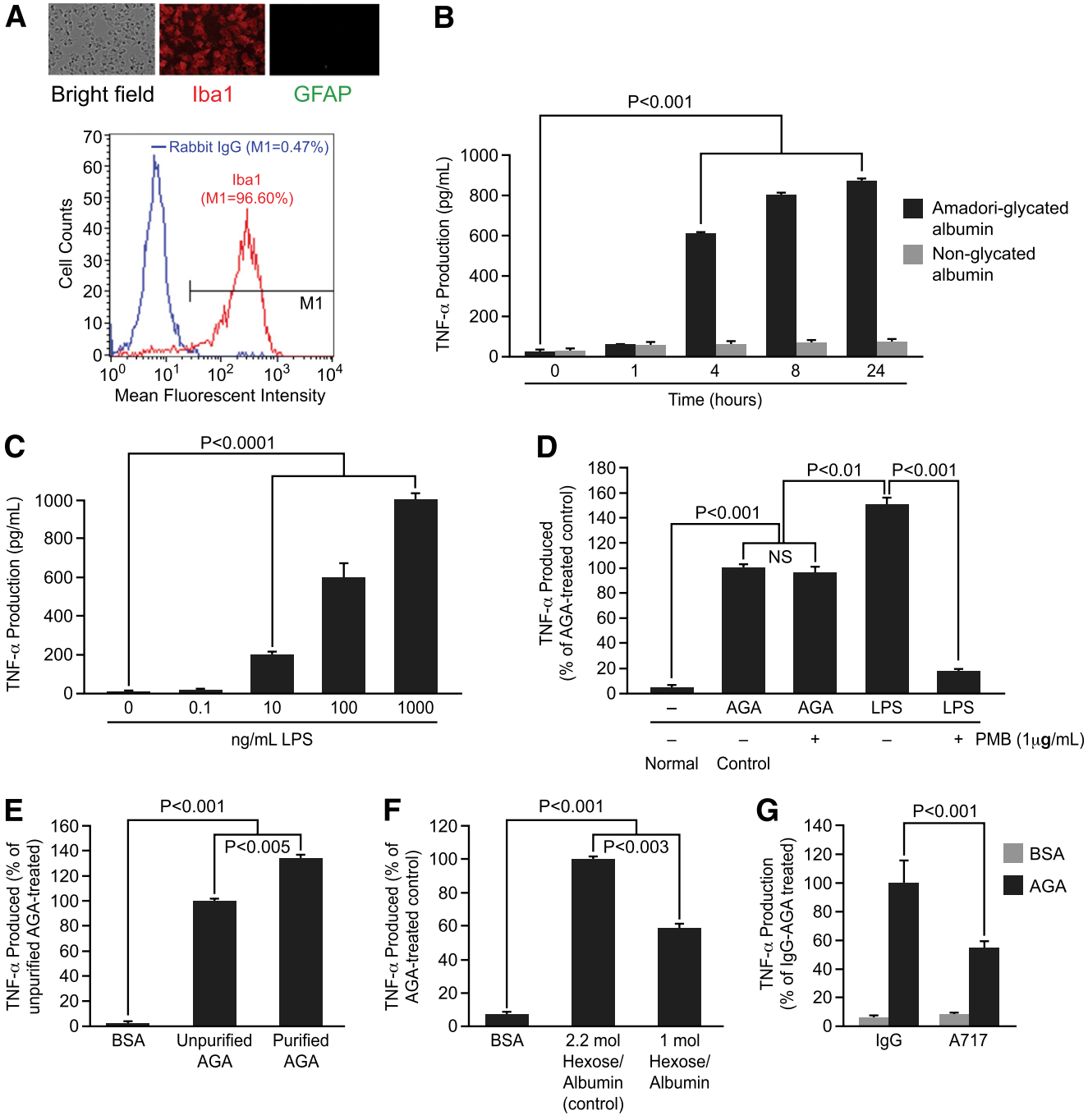

FIG. 3. AGA induces TNF-α release by retinal microglial cells in vitro. *A*: Characterization of retinal microglial cells by immunocytochemistry and flow cytometry. The panel contains a bright field view and immunodetection of Iba1 (red), GFAP (green), and flow cytometric analysis to determine cell purity. For flow cytometry analysis, cells with fluorescent intensity in M1 region were determined as positive for Iba1 and their percentage in the total population is shown. Normal rabbit IgG was used as control. *B*: Time-dependent release of TNF-α in AGA-treated retinal microglial cells. Cells were treated with AGA (500 μg/mL) or an equal level of nonglycated albumin for the indicated time. TNF-α levels in the culture media were measured by ELISA. Data shown are the mean ± SD of three experiments. *C–G*: TNF-α production in microglial cells after 4-h incubation with (*C*) purified lipopolysaccharide (0.1–1,000 ng/mL); (*D*) media containing 1 μg/mL LPS or 500 μg/mL AGA in the presence or absence of 1 μg/mL polymyxin B; (*E*) 500 μg/mL of BSA, unpurified, purified AGA; (*F*) 500 μg/mL of BSA, AGA with 2.2 mol hexose/albumin, or 1 mol hexose/albumin; (*G*) 500 μg/mL of BSA or AGA neutralized by A717 or IgG, which served as isotypic control. Data shown are the mean ± SD of three experiments. PBM, polymyxin B. (A high-quality color representation of this figure is available in the online issue.)

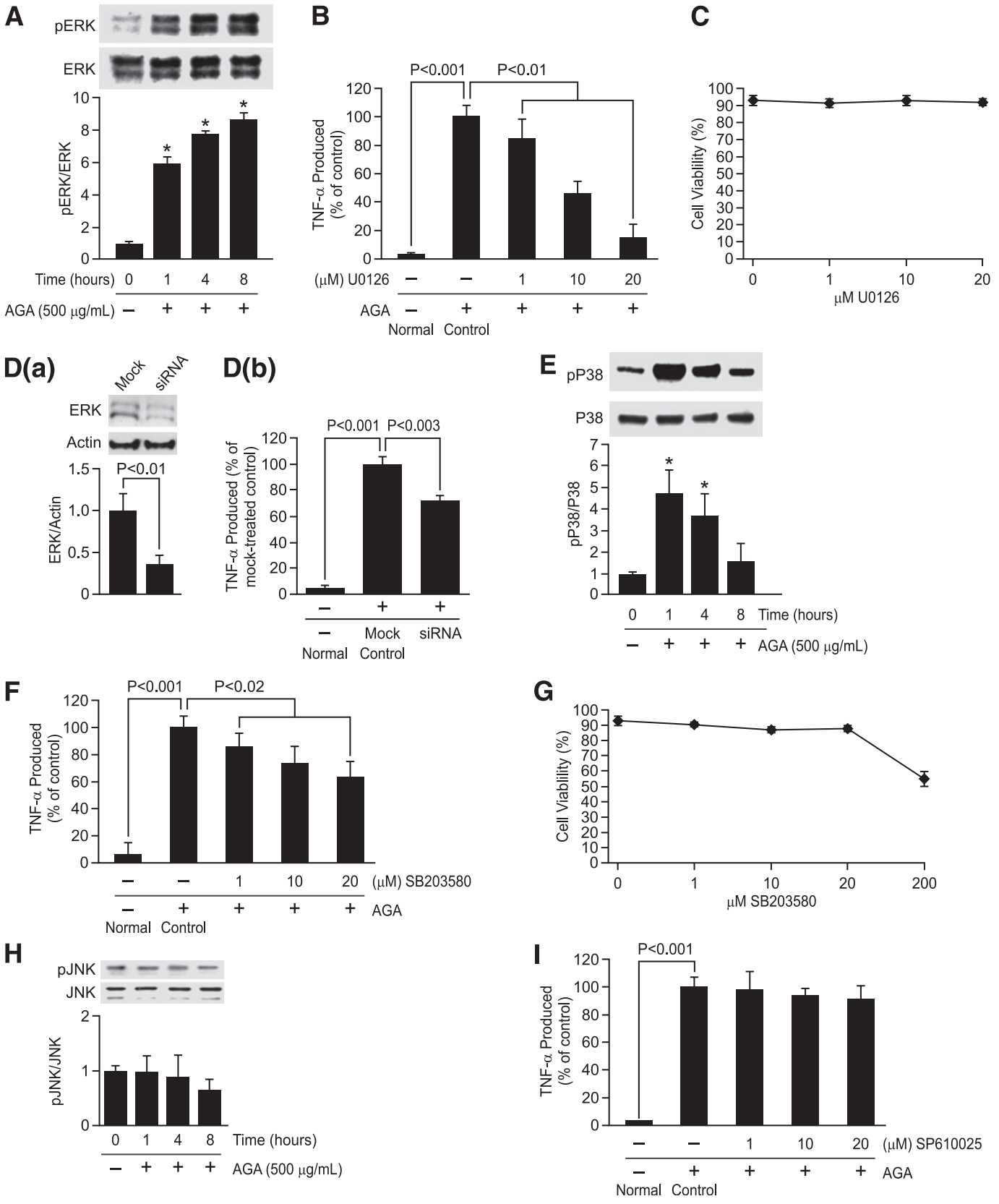

FIG. 4. Phosphorylation of ERK and P38, but not JNK, causes TNF-α release in the activated retinal microglial cells. *A*: Time-dependent, AGA-induced activation of ERK in retinal microglial cells. Cells were treated with 500 μg/mL AGA for 1–8 h. Phospho (p)ERK and its total protein in cell lysate were determined by Western analysis. Ratios of the intensities of phospho-proteins relative to total proteins for each time point were compared with control, which was arbitrarily set at 1.0. Data shown are the mean ± SD of three experiments (*$P < 0.001$). *B*: Dose-dependent inhibition of AGA-induced TNF-α release in retinal microglial cells by inhibitor for ERK (U0126). Cells were treated with 500 μg/mL of AGA for 4 h in the presence of indicated concentrations of inhibitor. TNF-α levels were compared with the vehicle-treated control. Data shown are the mean ± SD of three to five experiments. *C*: U0126 also had no effect on cell viability, as determined by trypan blue exclusion test. *D*: Inhibition of

AGA induces TNF-α release by retinal microglial cells in vitro. After having shown that AGA plays a role in diabetes-induced retinal inflammation, we next sought to dissect out the mechanism(s) responsible for the observed effect. Therefore, a cultured retinal microglia model was developed to characterize the microglial response to AGA treatment. The purity of this culture preparation was assessed by immunocytochemistry and flow cytometry. By immunocytochemistry, the majority was Iba1-positive, whereas the contaminating astrocytes were insignificant. By flow cytometry, the purity of microglia was 96.6% (Fig. 3*A*) and GFAP-positive cells were less than 1% (data not shown). With the use of this model, incubation with AGA (500 mg/mL) significantly stimulated TNF-α production starting at 4 h and remained elevated over the 24-h experimental period, whereas incubation with nonglycated albumin for 1–24 h had no effect (Fig. 3*B*). Moreover, there was nonsignificant cell death after 4 h of AGA treatment (Supplementary Fig. 3). To verify that the stimulatory effect of AGA on TNF-α release was mediated by glycated albumin only and not by endotoxin or any other contaminants, we first checked the endotoxin level in AGA solutions used in this study and confirmed to be endotoxin free (<0.125 units/mL, 10 endotoxin unit = 1 ng lipopolysaccharide). This estimated contamination of endotoxin was clearly below the threshold concentration of purified lipopolysaccharide (LPS) (0.1–10 ng/mL) required for a significant microglial stimulation (Fig. 3*C*). Moreover, to fully exclude the possible effects that any contaminating traces of endotoxin AGA still might have on the observed inflammatory response, we preincubated AGA-containing media with LPS-binding polymyxin B. At a concentration of 1 μg/mL, polymyxin B resulted in 90% inhibition of TNF-α production in microglia activated by purified LPS (1 μg/mL) without affecting cell viability (90–93% compared with 90–95% for controls). The incubation of AGA (500 μg/mL) with the same concentration of polymyxin B did not reduce the TNF-α production induced by AGA, whereas the overall TNF-α production was clearly smaller in AGA-incubated cells than that induced by purified LPS (Fig. 3*D*). Thus, the stimulatory effect of the AGA on TNF-α release from microglia is independent of contamination with endotoxin.

Second, to ensure that the AGA-mediated TNF-α release was indeed due to glycated albumin only and not to any contaminant that might be associated with the commercially available preparation, we compared the TNF-α–releasing ability of the purified AGA with that of the unpurified one. Purification of AGA, which resulted in a preparation with 70–75% yield, had a TNF-α–releasing activity 34 ± 3% higher than the unpurified one (Fig. 3*E*). Following this further, we tested the ability of an alternative AGA preparation, obtained from Exocell Inc., to elicit the inflammatory response in microglia. As shown in Fig. 3*F*, a significant increase in TNF-α level was seen after 4 h of incubation with this alternative product compared with nonglycated albumin. The amount of TNF-α released from microglia in response to glycated albumin varied with the degree of protein glycation as seen in these two alternative preparations. Last, to further confirm the specific effect of AGA on TNF-α production, the AGA-neutralizing antibody, A717, was used. The increase in TNF-α level mediated by AGA was reduced significantly by preincubation with A717, but not with IgG (Fig. 3*G*). Collectively, these results indicate that AGA induces TNF-α release by retinal microglial cells in vitro and that increase is indeed consecutive to a glycated albumin effect and not to species difference, endotoxin, or any other minor contaminants.

AGA-induced TNF-α release in retinal microglia is mediated by MAPKs. In light of AGA's inflammatory ability to induce TNF-α release by microglia, interest in the molecular mechanisms underlying this response has been expanded to include ERK, P38, and JNK MAPK pathways. Whether or not these kinases are involved in AGA-induced TNF-α release was investigated. Sustained elevation of ERK phosphorylation occurred over the 8-h experimental period (Fig. 4*A*), and that pattern is particularly indicative of its role in microglial response to AGA exposure. To determine the causal role of ERK in mediating TNF-α release, two approaches were used. First, an ERK inhibitor, U0126, significantly inhibited AGA-induced TNF-α release in a dose-dependent manner, without affecting cell viability (Fig. 4*B* and *C*). Second, microglia were transiently transfected with ERK siRNA or with scrambled siRNA and treated with AGA as before. ERK, but not scrambled siRNA, significantly inhibited TNF-α release (Fig. 4*D*, *a* and *b*).

Concomitant with ERK activation, phosphorylation of P38 occurred transiently at 1–4 h after AGA treatment (Fig. 4*E*). Because P38 has complicated species multiplicity, we used SB203580, a compound that inhibits P38 family of MAPK but not other MAP kinases (26), to study the causal role of p38 in mediating TNF-α release. SB203580 significantly inhibited TNF-α release without affecting cell viability (Fig. 4*F* and *G*). To confirm these results, another selective p38 inhibitor, SB202190, was also used. As did SB203580, SB202190 significantly reduced TNF-α production in a dose-dependent manner without affecting cell viability (Supplementary Fig. 4*A*–*C*). In contrast, phosphorylation of JNK remained unchanged over the entire experimental period (Fig. 4*H*), and its inhibitor (SP610025) did not inhibit AGA-induced TNF-α release (Fig. 4*I*). These results demonstrate that activation of ERK and P38, but not JNK, mediates AGA-induced TNF-α release in retinal microglia.

Crosstalk between ERK and P38 pathways in AGA-treated microglia. Next, we further determined any interaction between ERK and P38 pathways in the AGA-treated retinal microglia by examining the effect of P38 and ERK inhibitors on self and mutual activation. U0126, which blocks MEK, upstream of ERK, blocked the phosphorylation of both

AGA-induced TNF-α release by ERK siRNA in retinal microglial cells. Cells were transfected with siRNA or scrambled siRNA for 48 h and then treated with AGA for 4 h. *a*, Measurement of ERK expression relative to actin by Western blot after transfection with anti-ERK siRNA. Data shown are the mean ± SD of three experiments. *b*, ELISA-measured TNF-α levels were compared with the scrambled siRNA-transfected control. Data shown are the mean ± SD of three experiments. *E* and *H*: Time-dependent, AGA-induced activation of P38 and JNK in retinal microglial cells. Cells were treated with 500 μg/mL AGA for 1–8 h. Phospho (p)P38, pJNK, and its total proteins in cell lysates were determined by Western analysis. Ratios of the intensities of phospho-proteins relative to total proteins for each time points were compared with control, which was arbitrarily set at 1.0. Data shown are the mean ± SD of three experiments (*$P < 0.001$). *F* and *I*: Dose-dependent inhibition of AGA-induced TNF-α release in retinal microglial cells by inhibitors for P38 (SB203580) and JNK (SP610025). Cells were treated with 500 μg/mL of AGA for 4 h in the presence of indicated concentrations of inhibitors. TNF-α levels were compared with the vehicle-treated control. Data shown are the mean ± SD of three to five experiments. *G*: Effect of SB203580 on cell viability, as determined by trypan blue exclusion test.

ERK and P38 (Fig. 5*A*). In contrast, SB203580 increased the phosphorylation of both P38 and ERK. Further, we determined whether ERK and P38 both contributed to TNF-α release. Microglia were pretreated with U0126 and SB203580 individually or in combination and then activated by AGA. The combination of ERK and P38 inhibitors further inhibited TNF-α release than either one did individually (Fig. 5*B*).

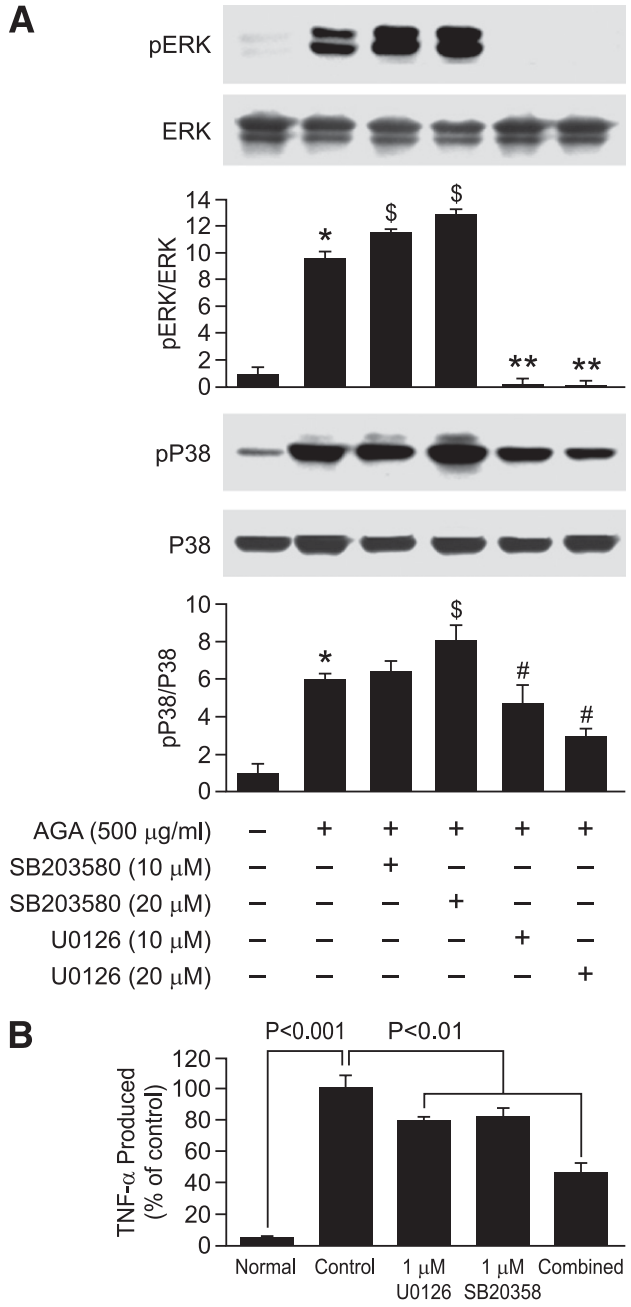

FIG. 5. Positive crosstalk occurs between ERK and P38 in AGA-treated retinal microglial cells. *A*: Effect of P38 and ERK inhibitors on AGA-induced MAP kinase activation. Cells were treated with AGA in the presence or absence of P38 inhibitor (SB203580) and ERK inhibitor (U0126) for 4 h. Phospho-ERK, total ERK, phospho-P38, and total P38 MAPK were determined as above. Each AGA-treated sample with or without inhibitors was compared with the untreated sample, set as 1.0. Data shown are the mean ± SD of three experiments. $$P < 0.05$; #$P < 0.05$; and **$P < 0.001$. *B*: Effect of individual vs. combined ERK and P38 inhibitors on TNF-α release. Cells were treated with U0126 or SB203580 alone or in combination for 30 min. Cells were then treated with AGA (500 μg/mL) for 4 h. TNF-α levels were compared with the vehicle-treated control. Data shown are the mean ± SD of three experiments.

AGA-induced reactive oxygen species formation causes MAPKs activation and TNF-α release in microglia. Despite these observations, the information regarding signal transduction from the microglial AGA receptor to ERK/P38-induced cytokine secretion remains largely unknown. Reactive oxygen species (ROS) production has been shown to be an early event induced in response to glycated protein stimulus (27). To test whether ROS is causally related to MAPKs-mediated TNF-α release, we first tested the contribution of ROS formation to AGA-induced TNF-α release. As shown in Fig. 6*A–C*, the inhibitory effects of an antioxidant, cannabidiol (CBD) (28), on ROS formation and TNF-α release without affecting cell viability demonstrate that ROS formation is a causative event in AGA-induced TNF-α release from microglia. Next, to determine whether ROS causally influenced MAPKs activation, phosphorylation of ERK and P38 was measured in AGA-treated microglia in the presence and absence of CBD. As shown in Fig. 6*D* and *E*, CBD significantly attenuated the phosphorylation of ERK and P38, indicating that oxidative stress is a common signaling event that is located upstream of both ERK/P38 pathways mediating TNF-α release in AGA-treated microglia.

DISCUSSION

Recent studies have shown that retinal inflammation is a relatively early event that occurs in the context of DR before vascular dysfunction (29–32). Microglial activation has been recognized as a potential culprit mechanism contributing to this early inflammatory outcome (3,24). However, the mechanism by which diabetes activates microglia to release inflammatory cytokines remains a critical missing link. If such a link is established, clinical interventions with agents that target these early features of DR would provide long-term vascular benefits. Hyperglycemia is still considered the principal cause of diabetes complications, and its deleterious effects are attributed, among other things, to the formation of the so-called AGA. In this study, we put forward a new concept pertaining to the involvement of AGA in the genesis of diabetes-induced retinal microglial activation and inflammation.

Microglia are sensitive to small changes in their environment, and they can be activated by a variety of factors, including proinflammatory cytokines, lipopolysaccharide, damaged cells, or any immune-stimulatory agents (33). Activated microglia have phagocytic and cytotoxic abilities to destroy foreign materials by secreting cytokines and other signaling molecules. However, if microglia remain in a sustained activated state, the secreted cytokines can affect other cell types in the proximity, particularly neuronal and vascular cells (34), bringing about the progression of many retinal diseases, including retinal degeneration (35) and glaucoma (36). Given these functions, microglial activation represents an important player in the pathogenesis of DR. This input has originated partly from histopathologic studies that show clustering of apparently activated microglia in the diabetic rat retina (37,38). These initial observations have been supported in postmortem human retinas (39) and reinforced by additional histopathologic studies showing that many inflammatory molecules, such as TNF-α, can be detected in the diabetic retina, often in association with microglia (24,40). The retinal expression of TNF-α has been reported to be associated with neuronal and endothelial cell

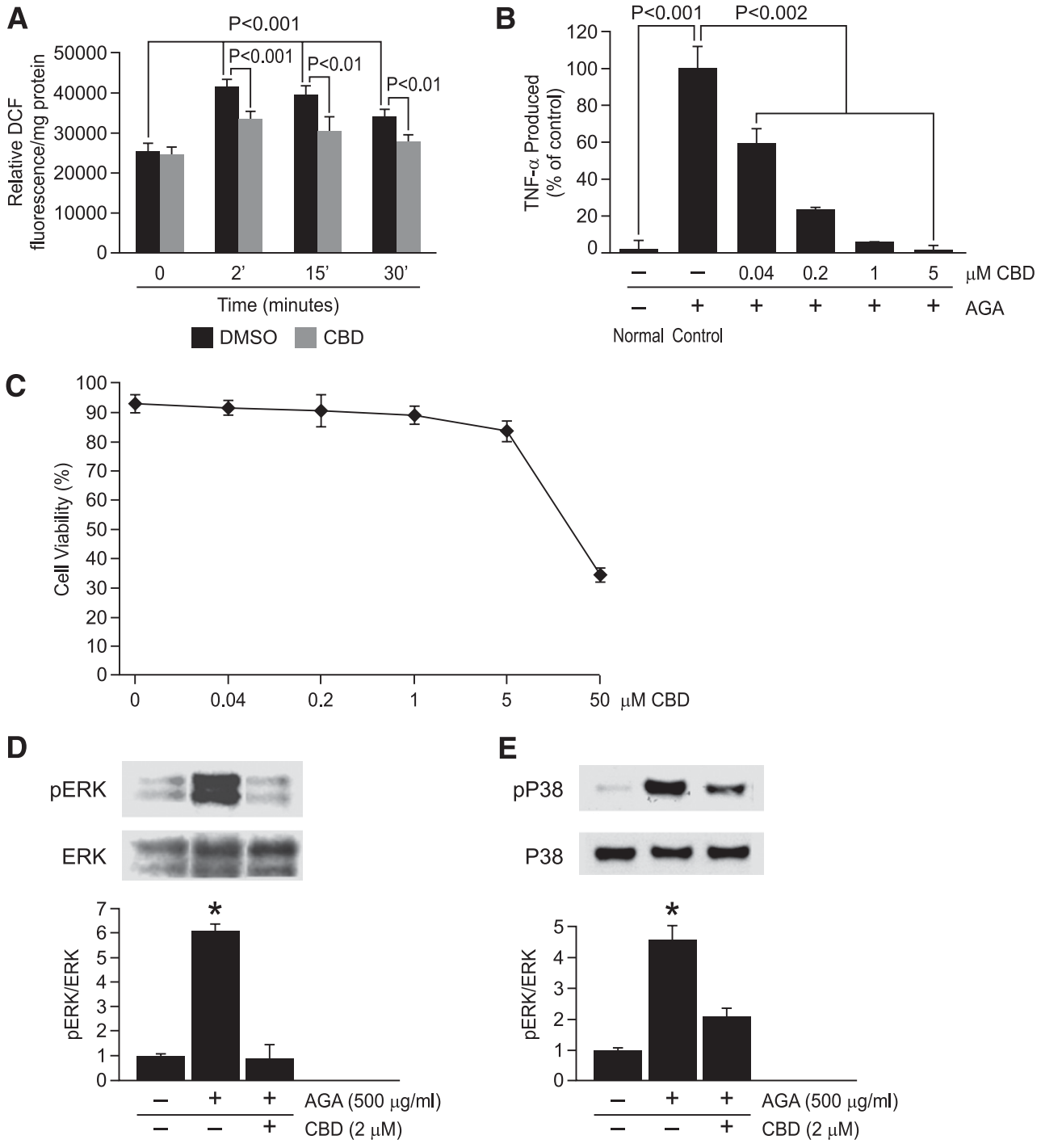

FIG. 6. ROS formation is an early event involved in AGA-induced TNF-α release and MAPKs activation in retinal microglial cells. *A*: AGA-induced, time-dependent ROS formation in retinal microglial cells. ROS formation was prevented by pretreatment with CBD (2 μmol/L). Retinal microglial cells loaded with 2′,7′-dichlorodihydrofluorescein diacetate were pretreated with CBD or DMSO for 60 min and treated with AGA, and the fluorescence of DCF was measured at 0, 2, 15, or 30 min. ROS formation was expressed as changes in DCF fluorescence/mg protein. Data shown are the mean ± SD of six experiments. *B*: Dose-dependent inhibition of AGA-induced TNF-α release in retinal microglial cells by CBD. Cells were treated with 500 μg/mL of AGA for 4 h in the presence of indicated concentrations of CBD. TNF-α levels were compared with the vehicle-treated control. *C*: Effect of CBD on cell viability, as determined by trypan blue exclusion test. Data shown are the mean ± SD of three experiments. *D* and *E*: CBD inhibits AGA-induced MAPKs activation in retinal microglial cells. Cells were treated with vehicle or CBD 30 min before AGA treatment for 4 h. Phospho-ERK, total ERK, phospho-P38, and total P38 MAPK were determined by Western blot and quantified by densitometric analyses. Each AGA-treated sample with or without inhibitors was compared with the untreated sample, set as 1.0. Data shown are the mean ± SD of three experiments. *$P < 0.001$.

death, hallmark features of the disease (41,42), and inhibition of TNF-α has demonstrated beneficial effects in the prevention of early DR (43). Moreover, the in vitro studies on co-cultured retinal neurons R28 with activated microglia have shown that microglia produce cytotoxins that kill retinal neuronal cells (3).

All of this seemingly overwhelming evidence has sculpted the concept of activated microglia as a contributing factor

in DR. Similar to microglia, macroglia are capable of assuming different morphologies and functions, reactive macrogliosis, in response to changes in their environment. In Mueller cells of the retina, de novo expression of GFAP is indicative of any kind of impairment of the retina, including experimental DR (44). This overexpression of Mueller GFAP starts to be obvious at 8 weeks of diabetes (45). Consistent with these previous studies, similar changes in morphology and antigen-expression patterns of retinal glial cells during diabetes were observed, such as hypertrophic microglia with increased expression of their markers and GFAP-positive Mueller cells. However, this study is the first to show that the acquisition of gliotic features within the diabetic retina was characterized by the activation of ERK and P38 exclusively in microglia but not in Mueller cells or astrocytes.

We then sought to determine what causes microglial activation and the accompanying increased inflammatory cytokines in the diabetic retina. One hypothesis that has been under investigation in other organs and has been raised by our initial Western and microscopic studies is AGA/inflammation cascade hypothesis. We have shown that AGA is increased in rats with diabetes compared with rats without diabetes and is localized in regions of microglial distribution. These findings, together with the observations that A717 significantly attenuated the expression of both Iba1 and TNF mRNA in 8-week diabetic rats and that intravitreal injection of AGA per se in normal rats induced Iba-1 expression and TNF-α release, have strengthened the notion that increased levels of AGA in the diabetic retina are an important contributor to microglial activation and thereby inflammation. The accumulation of AGA within the diabetic retina could be explained in part by the vascular leakage (Fig. 2*B*) that occurs early during experimental diabetes in the venules and capillaries of the superficial inner retinal vasculature (46). This vascular leakage promotes microvascular permeability and thereby enhances the direct contact of plasma-borne glycated albumin with the inner retinal layer, modulating the production of cytokines by microglia. However, the microvascular leakage is not the only contributor to the increased retinal AGA, and the possibility of local AGA formation cannot be ruled out (17).

Accordingly, the direct relationship between microglia and AGA has been explored through in vitro study. Wang et al. (27) reported that glycated proteins may alter microglia function by enhancing intracellular ROS formation and activating MAPKs-mediated TNF-α release but did not portray the causal relationship among these pathways. We expanded on that study and demonstrated two clear findings: AGA triggers the secretion of TNF-α, which is varied with the degree of protein glycation, and this inflammatory response is mediated by ROS and its subsequent signaling, ERK and P38 but not JNK MAPK. Furthermore, we broadened the scope to include the crosstalk between ERK and P38 pathways in microglia after AGA treatment. Inhibition of ERK by U0126 led to decreased phosphorylation of P38 MAPK, whereas blocking P38 phosphorylation by SB 203580 resulted in a reciprocal increase in the phosphorylation of ERK. In addition, even though SB 203580 is an inhibitor of p38 activity, it was also seen to increase p38 phosphorylation; although unexplained at this point, the observation has been reported (47). Similar to retinal microglia, concurrent activation of ERK and P38 occurs in melanoma, and the positive crosstalk between ERK and P38 in melanoma stimulates migration and in vivo proliferation (48). This positive crosstalk is in direct contrast with carcinoma cells in which the activity of the two kinases seems to be mutually exclusive (49). However, our results are not in agreement with the study by Wang et al. showing that the production of TNF-α was mediated by ERK, P38, and JNK (27). This discrepancy may be explained by the use of a different JNK inhibitor, curcumin (50 μmol/L), which shows a broad selectivity for various targets and is a potent scavenger of free radicals (50). Together, these inhibitor experiments point out that AGA-induced TNF-α is mediated by two alternative pathways partially interacting with each other. Figure 7 illustrates these pathways and the mechanism by which various drugs block these processes. Although these in vitro data provide a mechanistic paradigm whereby AGA induces microglial inflammatory response, used at nonphysiologic exposure condition (500 μg/mL), the relevance of these findings at lower AGA exposure levels needs to be further investigated.

Collectively, the experiments in this study provide new insights in understanding the pathogenesis of early features of DR, demonstrating that the accumulation of AGA within the diabetic retina elicits the microglial activation and secretion of TNF-α. In addition, our in vitro data disclose the molecular mechanisms involved therein, showing that AGA triggers TNF-α release from microglia in ROS and its subsequent ERK and P38 MAPKs-dependent mechanisms. Thus, clinical intervention trials with agents that neutralize glycated albumin effect might be warranted in modulating early pathologic pathways long before the occurrence of vision loss among patients with diabetes.

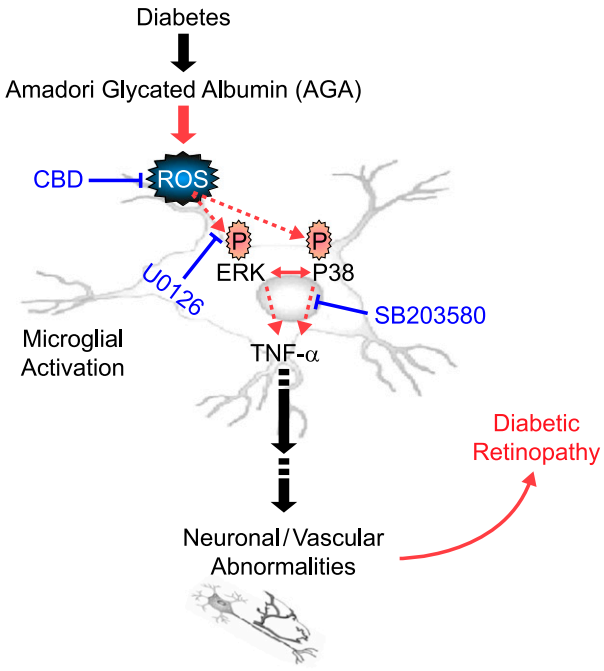

FIG. 7. Signaling pathways in the diabetes-induced retinal inflammation. Diabetes-induced AGA leads to ROS formation, activation of ERK/P38, and TNF-α release during microglial activation. Also included is the mechanism by which various drugs block these processes. (A high-quality color representation of this figure is available in the online issue.)

ACKNOWLEDGMENTS

This work was supported in part by Egyptian Culture and Education Bureau (A.S.I.), Knights Templar Educational Foundation, Vision Discovery Institute at the Medical College of Georgia, the American Diabetes Association (G.I.L.), and the Juvenile Diabetes Research Foundation (A.B.E. and W.Z.).

No potential conflicts of interest relevant to this article were reported.

A.S.I. researched data, contributed to discussion, wrote the article, and reviewed and edited the article. A.B.E. contributed to discussion and reviewed and edited the article. S.M. researched data. W.Z. researched data and contributed to discussion. Y.P., S.K., and M.M.A. contributed to discussion. M.M.E. contributed to discussion and reviewed and edited the article. G.I.L. researched data, contributed to discussion, wrote the article, and reviewed and edited the article.

The authors thank Ahmed El-Awady and Dr. Mohamed Al-Shabrawey of Medical College of Georgia, for assistance with the real-time PCR, and the anonymous reviewers, for constructive suggestions to improve the article. The authors dedicate this work to the memory of their colleague, Dr. Ahmed Rabie, who died in December 2009.

REFERENCES

1. Schalkwijk CG, Poland DC, van Dijk W, et al. Plasma concentration of C-reactive protein is increased in type I diabetic patients without clinical macroangiopathy and correlates with markers of endothelial dysfunction: evidence for chronic inflammation. Diabetologia 1999;42:351–357
2. Sjølie AK, Stephenson J, Aldington S, et al. Retinopathy and vision loss in insulin-dependent diabetes in Europe. The EURODIAB IDDM Complications Study. Ophthalmology 1997;104:252–260
3. Krady JK, Basu A, Allen CM, et al. Minocycline reduces proinflammatory cytokine expression, microglial activation, and caspase-3 activation in a rodent model of diabetic retinopathy. Diabetes 2005;54:1559–1565
4. Negre-Salvayre A, Salvayre R, Augé N, Pamplona R, Portero-Otín M. Hyperglycemia and glycation in diabetic complications. Antioxid Redox Signal 2009;11:3071–3109
5. Sabbatini M, Sansone G, Uccello F, Giliberti A, Conte G, Andreucci VE. Early glycosylation products induce glomerular hyperfiltration in normal rats. Kidney Int 1992;42:875–881
6. Naitoh T, Kitahara M, Tsuruzoe N. Tumor necrosis factor-alpha is induced through phorbol ester—and glycated human albumin-dependent pathway in THP-1 cells. Cell Signal 2001;13:331–334
7. Amore A, Cirina P, Mitola S, et al. Nonenzymatically glycated albumin (Amadori adducts) enhances nitric oxide synthase activity and gene expression in endothelial cells. Kidney Int 1997;51:27–35
8. Cohen MP, Shea E, Shearman CW. ERK mediates effects of glycated albumin in mesangial cells. Biochem Biophys Res Commun 2001;283:641–643
9. Brandt R, Krantz S. Glycated albumin (Amadori product) induces activation of MAP kinases in monocyte-like MonoMac 6 cells. Biochim Biophys Acta 2006;1760;1749–1753
10. Higai K, Shimamura A, Matsumoto K. Amadori-modified glycated albumin predominantly induces E-selectin expression on human umbilical vein endothelial cells through NADPH oxidase activation. Clin Chim Acta 2006; 367:137–143
11. Chen S, Cohen MP, Ziyadeh FN. Amadori-glycated albumin in diabetic nephropathy: pathophysiologic connections. Kidney Int Suppl. 2000;77: S40–S44
12. Rodríguez-Mañas L, Angulo J, Vallejo S, et al. Early and intermediate Amadori glycosylation adducts, oxidative stress, and endothelial dysfunction in the streptozotocin-induced diabetic rats vasculature. Diabetologia 2003;46:556–566
13. Pu LJ, Lu L, Shen WF, et al. Increased serum glycated albumin level is associated with the presence and severity of coronary artery disease in type 2 diabetic patients. Circ J 2007;71:1067–1073
14. Schalkwijk CG, Ligtvoet N, Twaalfhoven H, et al. Amadori albumin in type 1 diabetic patients: correlation with markers of endothelial function, association with diabetic nephropathy, and localization in retinal capillaries. Diabetes 1999;48:2446–2453
15. Tang J, Zhu XW, Lust WD, Kern TS. Retina accumulates more glucose than does the embryologically similar cerebral cortex in diabetic rats. Diabetologia 2000;43:1417–1423
16. Clements RS Jr, Robison WG Jr, Cohen MP. Anti-glycated albumin therapy ameliorates early retinal microvascular pathology in db/db mice. J Diabetes Complications 1998;12:28–33
17. Cohen MP, Hud E, Wu VY, Shearman CW. Amelioration of diabetes-associated abnormalities in the vitreous fluid by an inhibitor of albumin glycation. Invest Ophthalmol Vis Sci 2008;49:5089–5093
18. El-Remessy AB, Khalil IE, Matragoon S, et al. Neuroprotective effect of (-) Delta9-tetrahydrocannabinol and cannabidiol in N-methyl-D-aspartate-induced retinal neurotoxicity: involvement of peroxynitrite. Am J Pathol 2003;163:1997–2008
19. Shen WY, Garrett KL, Wang CG, et al. Preclinical evaluation of a phosphorothioate oligonucleotide in the retina of rhesus monkey. Lab Invest 2002;82:167–182
20. El-Remessy AB, Tang Y, Zhu G, et al. Neuroprotective effects of cannabidiol in endotoxin-induced uveitis: critical role of p38 MAPK activation. Mol Vis 2008;14:2190–2203
21. Miele C, Riboulet A, Maitan MA, et al. Human glycated albumin affects glucose metabolism in L6 skeletal muscle cells by impairing insulin-induced insulin receptor substrate (IRS) signaling through a protein kinase C alpha-mediated mechanism. J Biol Chem 2003;278:47376–47387
22. Cohen MP, Wu VY, Cohen JA. Glycated albumin stimulates fibronectin and collagen IV production by glomerular endothelial cells under normoglycemic conditions. Biochem Biophys Res Commun 1997;239:91–94
23. Cohen M. *Diabetes and Protein Glycation. Clinical and Pathophysiologic Relevance*. Philadelphia, PA, JC Press, 1996
24. Yang LP, Sun HL, Wu LM, et al. Baicalein reduces inflammatory process in a rodent model of diabetic retinopathy. Invest Ophthalmol Vis Sci 2009;50: 2319–2327
25. Nevado J, Peiró C, Vallejo S, et al. Amadori adducts activate nuclear factor-kappaB-related proinflammatory genes in cultured human peritoneal mesothelial cells. Br J Pharmacol 2005;146:268–279
26. Wilson KP, McCaffrey PG, Hsiao K, et al. The structural basis for the specificity of pyridinylimidazole inhibitors of p38 MAP kinase. Chem Biol 1997;4:423–431
27. Wang AL, Yu AC, He QH, Zhu X, Tso MO. AGEs mediated expression and secretion of TNF alpha in rat retinal microglia. Exp Eye Res 2007;84:905–913
28. Hampson AJ, Grimaldi M, Axelrod J, Wink D. Cannabidiol and (-)Delta9-tetrahydrocannabinol are neuroprotective antioxidants. Proc Natl Acad Sci U S A 1998;95:8268–8273
29. Zheng L, Howell SJ, Hatala DA, Huang K, Kern TS. Salicylate-based anti-inflammatory drugs inhibit the early lesion of diabetic retinopathy. Diabetes 2007;56:337–345
30. Abu El-Asrar AM, Desmet S, Meersschaert A, Dralands L, Missotten L, Geboes K. Expression of the inducible isoform of nitric oxide synthase in the retinas of human subjects with diabetes mellitus. Am J Ophthalmol 2001;132:551–556
31. Joussen AM, Poulaki V, Le ML, et al. A central role for inflammation in the pathogenesis of diabetic retinopathy. FASEB J 2004;18:1450–1452
32. Kern TS, Barber AJ. Retinal ganglion cells in diabetes. J Physiol 2008;586: 4401–4408
33. Aloisi F. Immune function of microglia. Glia 2001;36:165–179
34. Wood P. *Neuroinflammation: Mechanisms and Management*. Totowa, NJ, Humana Press, 2003
35. Yang LP, Li Y, Zhu XA, Tso MO. Minocycline delayed photoreceptor death in rds mice through iNOS-dependent mechanism. Mol Vis 2007;13:1073–1082
36. Bosco A, Inman DM, Steele MR, et al. Reduced retina microglial activation and improved optic nerve integrity with minocycline treatment in the DBA/2J mouse model of glaucoma. Invest Ophthalmol Vis Sci 2008;49:1437–1446
37. Zeng XX, Ng YK, Ling EA. Neuronal and microglial response in the retina of streptozotocin-induced diabetic rats. Vis Neurosci 2000;17:463–471
38. Rungger-Brändle E, Dosso AA, Leuenberger PM. Glial reactivity, an early feature of diabetic retinopathy. Invest Ophthalmol Vis Sci 2000;41:1971–1980
39. Zeng HY, Green WR, Tso MO. Microglial activation in human diabetic retinopathy. Arch Ophthalmol 2008;126:227–232
40. Liu W, Xu GZ, Jiang CH, Da CD. Expression of macrophage colony-stimulating factor (M-CSF) and its receptor in streptozotocin-induced diabetic rats. Curr Eye Res 2009;34:123–133
41. Joussen AM, Doehmen S, Le ML, et al. TNF-alpha mediated apoptosis plays an important role in the development of early diabetic retinopathy and long-term histopathological alterations. Mol Vis 2009;15:1418–1428

42. El-Remessy AB, Al-Shabrawey M, Khalifa Y, Tsai NT, Caldwell RB, Liou GI. Neuroprotective and blood-retinal barrier-preserving effects of cannabidiol in experimental diabetes. Am J Pathol 2006;168:235–244
43. Joussen AM, Poulaki V, Mitsiades N, et al. Nonsteroidal anti-inflammatory drugs prevent early diabetic retinopathy via TNF-alpha suppression. FASEB J 2002;16:438–440
44. Lieth E, Barber AJ, Xu B, et al.; Penn State Retina Research Group. Glial reactivity and impaired glutamate metabolism in short-term experimental diabetic retinopathy. Diabetes 1998;47:815–820
45. Yu X, Xu Z, Mi M, et al. Dietary taurine supplementation ameliorates diabetic retinopathy via anti-excitotoxicity of glutamate in streptozotocin-induced Sprague-Dawley rats. Neurochem Res 2008;33:500–507
46. Qaum T, Xu Q, Joussen AM, et al. VEGF-initiated blood-retinal barrier breakdown in early diabetes. Invest Ophthalmol Vis Sci 2001;42:2408–2413
47. Moon SE, Bhagavathula N, Varani J. Keratinocyte stimulation of matrix metalloproteinase-1 production and proliferation in fibroblasts: regulation through mitogen-activated protein kinase signalling events. Br J Cancer 2002;87:457–464
48. Estrada Y, Dong J, Ossowski L. Positive crosstalk between ERK and p38 in melanoma stimulates migration and in vivo proliferation. Pigment Cell Melanoma Res 2009;22:66–76
49. Aguirre-Ghiso JA, Estrada Y, Liu D, Ossowski L. ERK(MAPK) activity as a determinant of tumor growth and dormancy; regulation by p38(SAPK). Cancer Res 2003;63:1684–1695
50. Thangapazham RL, Sharma A, Maheshwari RK. Multiple molecular targets in cancer chemoprevention by curcumin. AAPS J 2006;8:E443–E449